Interactions of a Detonation Wave Confined by a High-Temperature Compressible Layer

REYNAUD Maxime, VIROT Florent, CHINNAYYA Ashwin
Institut PPRIME, UPR 3346 CNRS ENSMA
86961 Futuroscope-Chasseneuil Cedex, France

1 Introduction

The very rapid energy conversion leads to consider the detonation as an alternative to the classical constant pressure combustion in engines. However, many issues arise from its potential use for aeronautical propulsion applications because of the strongly non-ideal conditions of propagation endured by the detonation waves. Particularly in the rotating detonation engines (RDE), the detonation chamber is curved, the fresh mixture exhibits composition as well as temperature inhomogeneities and is confined by the burnt gases. The present work focuses on the effects induced by a high-temperature gaseous layer on the detonation propagation.

The presence of a yielding confinement affects the dynamics of the detonation [1–3]. The divergence of the streamlines downsteam of the front results in a velocity deficit and to its curvature. The ratio of acoustic impedances between the reactive and the inert layers influences the structure of the combined wave formed by the detonation and the oblique shock. Adams [4] experimentally showed that this parameter may lead to the appearance of a new topology characterized by the presence of a detached shock. This was also addressed in the calculations of Fievishon [5]. To assess whether this parameter may influence the detonation dynamics, we performed numerical simulations of a detonation confined by an inert layer at different temperatures and for mixtures of various stability. The simulations show qualitative agreement with the experimental literature. The losses endured by the detonation affect the mean profiles and the hydrodynamic thickness. The temperature of the inert layer acts in a non-negligible way on the detonation dynamics and modifies its propagation limits.

2 Governing Equations

The gas dynamics evolution is governed by the following reactive Euler equations :

$$\frac{\partial U}{\partial t} + \frac{\partial F(U)}{\partial x} + \frac{\partial G(U)}{\partial y} = S(U) \tag{1}$$

Correspondence to: ashwin@ensma.fr

with the conservative variables $U = (\rho, \rho u, \rho v, \rho E, \rho Y)$, the x-conservative flux $F = (\rho u, \rho u^2 + P, \rho uv, (\rho E + P)u, \rho Y u)$, the y-conservative flux $G = (\rho v, \rho uv, \rho v^2 + P, (\rho E + P)v, \rho Y v)$ and the source term $S = (0, 0, 0, 0, -\rho\dot{\omega})$. ρ is the density, P the pressure, u, v are the velocity components along the horizontal and vertical coordinates respectively. Y is the progress variable of the chemical reaction and ranges from 0 in the fresh gases to 1 in the detonation products. Assuming a perfect gas law, the total energy reads $E = e + \frac{u^2+v^2}{2} - Yq$, with q and γ the heat release and the ratio of specific heats, respectively. A one-step irreversible reaction is used to model the chemical process $\dot{\omega} = k(1 - Y)\exp\left(\frac{-E_a}{RT}\right)$. The reaction was artificially inhibited when the mass fraction reaches the value of $\epsilon = 10^{-3}$ in order to ensure that the reaction length remained finite.

3 Numerical methods and problem statement

We employed a classical time-operator splitting method with a directional splitting. The characteristic variables were reconstructed on the cell boundaries using a 9^{th} Monotonicity Preserving interpolation [6]. The fluxes through the interfaces were computed by solving the Riemann problem by means of the approximate HLLC solver [7]. The temporal-integration was accomplished using a third-order TVD explicit Runge-Kutta method. The parallelization of the code was achieved through a domain decomposition method with the MPI library. The largest simulations were performed on 480 processors with a typical cost of about 80,000 CPU scalar hours. A recycling process [8, 9] has been implemented in order to perform the computation on smaller domains, as well as a static mesh refinement method, with finer cells near the shock. The numerical resolution consisted of $N_{1/2} = 30$ points per half-reaction length, except for the mixture with $E_a/RT_0 = 38.23$ where the size of the computational domain needs to be enlarged and thus prevents from using such a resolution. For this case, $N_{1/2}$ was lowered to $N_{1/2} = 10$. Although this resolution seems low for such mildly unstable detonations, the average pressure $\overline{p}$ and Mach number $\widetilde{M}$ calculated in a convergence study with $N_{1/2} = 15$ and 20 agree well with each other. The conclusions of this study are thus not called into question relatively to this issue. The detonation propagates into a medium at rest composed of a gaseous reactive layer bounded by an inert gas on the top and by a wall at the bottom (see Figure 1). The detonation was initiated by setting an area at the von Neumann state, region located in the middle of the domain in the x direction and as high as the reactive layer. Then, the flow gradually evolved to reached a quasi-steady propagation independent from the ignition and the initial conditions. The front curvature increased progressively as the high-pressure products expanded toward the upper layer. Hydrodynamic instabilities appeared on the interface between the burnt gases and the inert gas. According to the intrinsic characteristic of the inert layer, an oblique or detached shock developed in the upper region. Transverses instabilities arose and gave birth to the cellular structure.

The thermodynamic parameters were chosen to be approximately those of a stoichiometric hydrogen/oxygen mixture at the initial pressure of 1 atm and the initial temperature of $T_0 = 295$ K. The ratio of specific heats and the heat release are given by $\gamma = 1.333$ and $q = 4.867$ MJ/kg, i.e. $q/rT_0 = 23.81$, respectively [10]. Corresponding CJ and von Neumann (vN) parameters are $D_{\text{CJ}} = 2845$ m/s, $P_{\text{CJ}} = 17.5$ bar, $T_{\text{CJ}} = 3007$ K, $P_{\text{vN}} = 34.0$ bar and $T_{\text{vN}} = 1707$ K. The temperature of the inert layer T_i was set at the beginning of each computation. Three different values of T_i were used : 295 K, which is the same temperature as the reactive layer in every simulations, 750 K and 1400 K. Moreover, three different values of the reduced activation energy E_a/RT_0 were employed in this study: 20, 30 and 38.23, the latter corresponding to the $2H_2 + O_2$ mixture [10]. The pre-exponential factor of the Arrhenius law was calculated in order to ensure that the half-reaction length $l_{1/2}$ remained identical in all cases ($l_{1/2} = 9.079 \times 10^{-5}$ m). In this abstract, only the

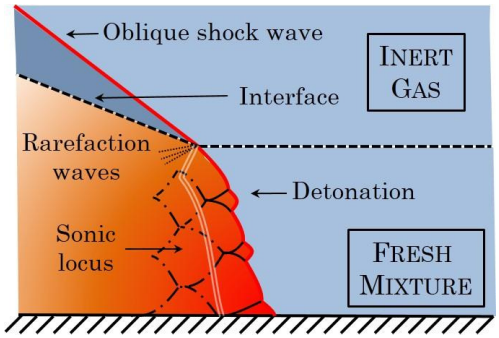

Figure 1: Schematic of the numerical configuration.

results for $E_a/RT_0 = 20$ will be presented.

4 Results and discussions

The Figure 2 presents the temperature fields for $T_i = 295$ K (a) and $T_i = 1400$ K (b). These results were obtained for a mixture with $E_a/RT_0 = 20$, ensuring a stable behavior. In this case $\lambda = 19\ l_{1/2}$ (≈ 2 mm), with λ the cell size without losses (at CJ velocity). For the configuration where the reactive and inert layers were at the same temperature (see Figure 2 (a)), one may observe the characteristic features of the semi-confined detonation: the curved front, the oblique shock and the interface between the inert and burnt gases. Transverse waves evolve downstream of the front, which are at the root of the cellular structure of the detonation and are clearly visible along the front. The irregularities on the interface are due to the upward motion of the triple points across the boundary between the inert and reactive layers. Because of the expansion of the burnt gases toward the upper compressible layer, the detonation is experiencing losses, which lead to a velocity deficit of 4% for the configuration of Figure 2 (a).

The Figures 2 (b) and (c) depict a configuration in which the upper layer is at 1400 K. This induces important modifications of the combined wave structure. First of all, the oblique shock angle increases drastically and a detached shock emerges near the junction with the detonation wave. A small oblique shock appears in the lower layer at the intersection between the detonation and the detached shock. The length of this shock oscillates according to the transverse waves propagation. A jet of fresh gases forms and is rolled up by the vortexes present near the interface between the detonation products and the inert gases. This jet is periodically shocked by the transverse waves and is then detached from the combined-wave structure when a triple point impacts the interface. As compared to the case with $T_i = 295$ K, the curvature of the front is less pronounced and the velocity deficit is lower (2.3%). The superposition of instantaneous combined wave profiles is exposed in the Figure 2 (d) for $T_i = 295$ K and $T_i = 1400$ K. The black curves correspond to the average shape of the front. With $T_i = 1400$ K, the detached shock is present on the instantaneous as well as on the mean profiles. Moreover, the curvature is reduced and the regularity increases.

The cellular structure is also strongly influenced by the inert layer temperature (see Figure 3). Each Figure corresponds to a different temperature T_i: 295 K (a), 750 K (b) and 1400 K (c). For the configuration with identical temperatures (a), the cellular structure is slightly irregular with an enlarged spectrum of the cell sizes. The increase of the confinement temperature leads to a more regular cellular structure. The impact of the triple points on the interface between the two layers give rise to a reflected wave. This phenomenon

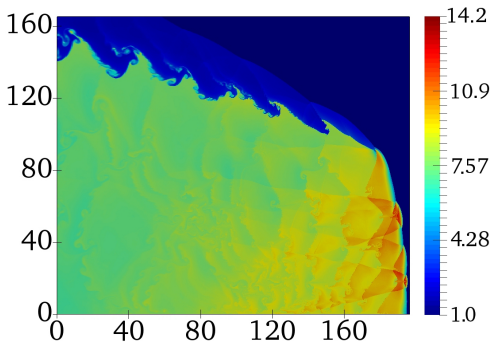

(a) $T_i = 295$ K

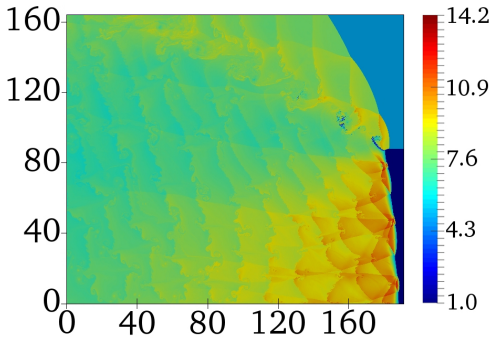

(b) $T_i = 1400$ K

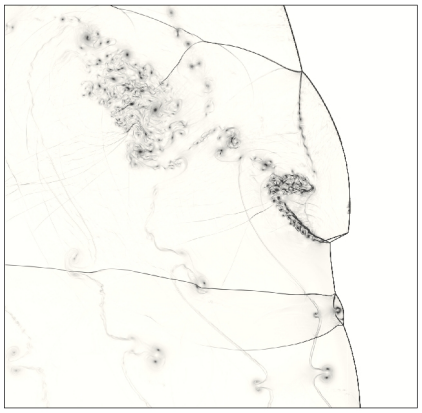

(c) $T_i = 1400$ K

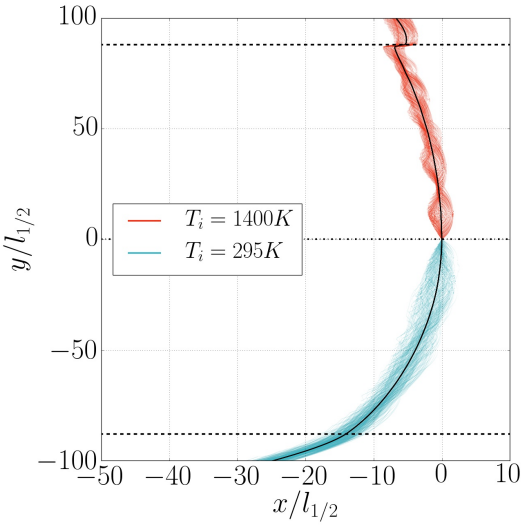

(d)

Figure 2: Normalized temperature fields obtained for $T_i = 295$ K (a) and $T_i = 1400$ K (b) with $E_a/RT_0 = 20$. The spatial dimensions are normalized by $l_{1/2}$. Figure (c): Schlieren of the density field for $T_i = 1400$ K (enlargement), presence of the detached shock. Figure (d): superposition of instantaneous combined wave profiles for $T_i = 295$ K and $T_i = 1400$ K.

constitutes a source of triple point regeneration on the contrary to the configuration (a). Indeed, in this case, no reflection of the transverse waves occurs at the interface between the inert and the reactive layer, and thus the only source of triple point regeneration relies on the intrinsic instabilities of the reactive flow field.

The deficit of velocity endured by the detonation as a function of the reactive layer height h is plotted in the Figure 4 for several temperatures of the inert confinement. As the reactive layer height is smaller, the velocity deficit increases. However, the high-temperature inert layer aims to reduce this deficit. This effect is more pronounced for the smallest reactive layers. For this mixture characterized by a low activation energy, this reduction of the velocity deficit may be linked to the decrease of the front curvature. The Figure 5 depicts the averaged evolution of the pressure downstream of the front as well as the mean hydrodynamic thickness for the different temperatures T_i. This averaging process took place along the bottom line of the domain $y = 0$ in the instantaneous shock coordinates. The increase of the inert layer temperature leads to higher pressures on the whole profile and to a slight lengthening of the hydrodynamic thickness.

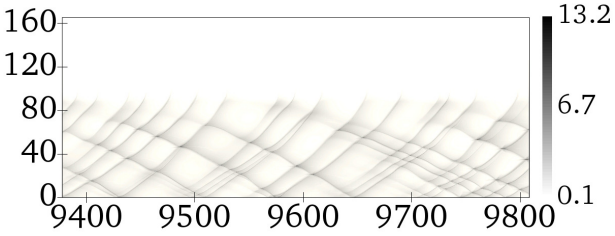

(a) $T_i = 295$ K

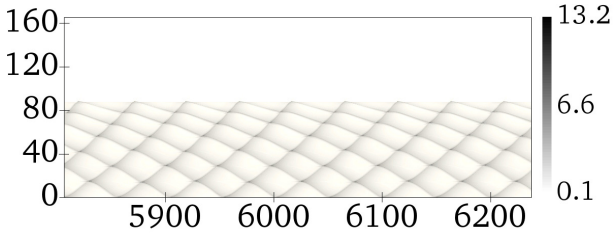

(b) $T_i = 750$ K

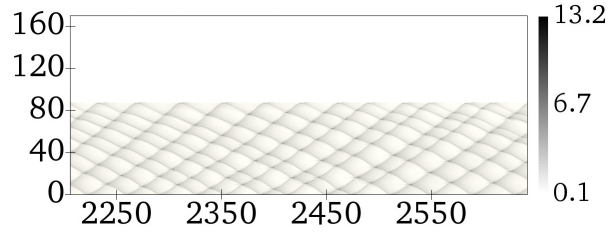

(c) $T_i = 1400$ K

Figure 3: Maximum pressure field illustrating the cellular structure for $E_a/RT_0 = 20$ and for different temperatures of confinement. The reactive layer height is $h = 88\ l_{1/2}$. The spatial dimensions are normalized by $l_{1/2}$ and the pressure is given in MPa.

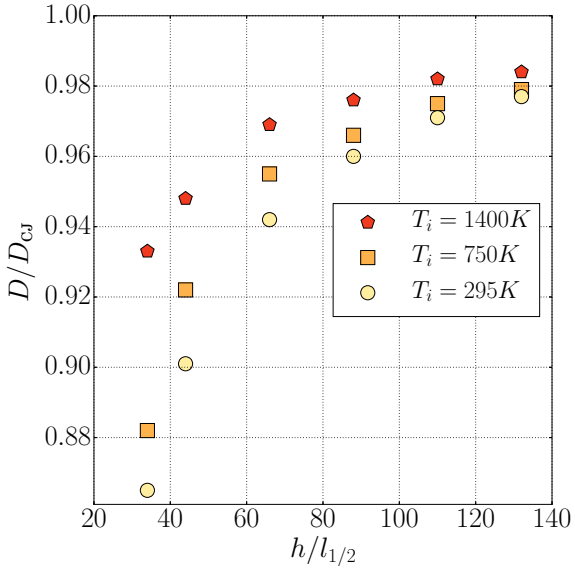

Figure 4: Mean velocity deficit of the detonation front as a function of the height of the reactive layer normalized by the half-reaction length for different temperatures of the inert confinement and for $E_a/RT_0 = 20$.

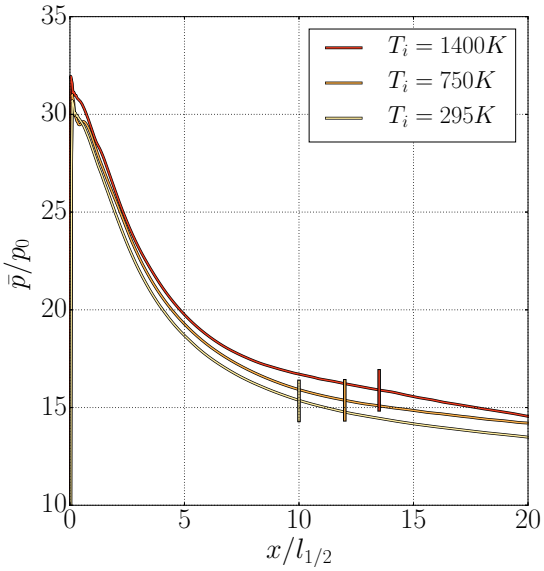

Figure 5: Average pressure profile as a function of the distance from the front normalized by the half-reaction length for different temperatures of the inert confinement and for $E_a/RT_0 = 20$. The vertical lines symbolize the mean localization of the mean sonic plane for the different temperatures. The reactive layer height is $h = 88\ l_{1/2}$.

5 Conclusion

In the current study, 2-D numerical simulations have been performed to study the influence of a compressible layer over the detonation propagation, and more specifically the influence of the temperature of this inert confinement. The results have shown that this parameter strongly affects the detonation, whether it be in its structure or its propagation. Indeed, for high-temperature confinements, the combined detonation wave differs from what is usually observed and a detached shock under which evolves a slight oblique shock appears. Moreover, the increase of the inert layer temperature strengthens the detonation by reducing its velocity deficit and by extending the limits of propagation. These findings demonstrate the significance of the yielding confinement nature on the detonation propagation. Further results concerning higher activation energies and the associated instabilities are under investigation and will be presented. The relation between the detonation velocity and its curvature will also be discussed.

Acknowledgements: The computations were performed using HPC resources from the cluster of PPRIME, the MÉSOCENTRE DE CALCUL POITEVIN and from GENCI-CINES (Grant 2016-c20162b7735). This work is part of the CAPA research program on Alternative Combustion Mode for air-breathing Propulsion supported by SAFRAN Tech, MBDA France and ANR (French National Research Agency).

References

[1] Dabora, E. K., Nicholls, J. A., and Morrison, R. B. "The influence of a compressible boundary on the propagation of gaseous detonations". 10th Symposium (International) on Combustion 10.1 (1965), pp. 817 –830.

[2] Vasil'ev, A. A. and Zak, D. V. "Detonation of gas jets". Combustion, Explosion and Shock Waves 22.4 (1986), pp. 463–468.

[3] Reynaud, M., Virot, F., and Chinnayya, A. "A computational study of the interaction of gaseous detonations with a compressible layer". Physics of Fluids 29.5 (2017), p. 056101.

[4] Adams, T. G. "Do Weak Detonation Waves Exist?" AIAA Journal 16.10 (1978), pp. 1035–1040.

[5] Fievisohn, R. and Yu, K. "Method of characteristic analysis of gaseous detonations bounded by an inert gas". Proceedings of the 25th ICDERS, Leeds (2015).

[6] Suresh, A and Huynh, H. T. "Accurate monotonicity-preserving schemes with RungeKutta time stepping". Journal of Computational Physics 136.1 (1997), pp. 83 –99.

[7] Toro, E. F., Spruce, M., and Speares, W. "Restoration of the contact surface in the HLL-Riemann solver". Shock Waves 4.1 (1994), pp. 25–34.

[8] Sow, A., Chinnayya, A., and Hadjadj, A. "Mean structure of one-dimensional unstable detonations with friction". Journal of Fluid Mechanics 743 (2014), pp. 503–533.

[9] Li, J., Mi, X., and Higgins, A. J. "Geometric scaling for a detonation wave governed by a pressure-dependent reaction rate and yielding confinement". Physics of Fluids 27.2 (2015).

[10] Gamezo, V. N., Desbordes, D., and Oran, E. S. "Two-dimensional reactive flow dynamics in cellular detonation waves". Shock Waves 9.1 (1999), pp. 11–17.